

Theory of triangular lattice quasi-one-dimensional charge-transfer solids

R. T. Clay*

*Department of Physics & Astronomy and HPC² Center for Computational Sciences,
Mississippi State University, Mississippi State, MS 39762*

N. Gomes and S. Mazumdar

Department of Physics, University of Arizona, Tucson, AZ 85721

(Dated: today)

Recent investigations of the magnetic properties and the discovery of superconductivity in quasi-one-dimensional triangular lattice organic charge-transfer solids have indicated the severe limitations of the effective $\frac{1}{2}$ -filled band Hubbard model for these and related systems. We present computational studies within the $\frac{1}{4}$ -filled band Hubbard model for these highly anisotropic systems. Individual organic monomer molecules, and not their dimers, constitute the sites of the Hamiltonian within our theory. We find enhancement of the long-range component of superconducting pairing correlations by the Hubbard repulsive interaction U for band parameters corresponding to κ -(BEDT-TTF)₂CF₃SO₃, which is superconducting under moderate pressure. We find significantly weaker superconducting pairing at realistic values of U in κ -(BEDT-TTF)₂B(CN)₄, and we ascribe the experimentally observed transition to a spin-gapped insulator to the formation of a paired-electron crystal. We make the testable prediction that the spin gap will be accompanied by charge-ordering and period doubling in two lattice directions. The weaker tendency to superconductivity in κ -(BEDT-TTF)₂B(CN)₄ compared to κ -(BEDT-TTF)₂CF₃SO₃ is consistent with the more one-dimensional character of the former. Pressure-induced superconductivity is, however, conceivable. The overall results support a valence bond theory of superconductivity we have proposed recently.

I. INTRODUCTION

Determination of the mechanism of correlated-electron superconductivity (SC) continues to be a formidable challenge, even after three decades of intensive investigations following the discovery of the phenomenon in doped copper oxides. Discoveries of many other exotic superconductors subsequently have only added to its mystique. One opinion, shared by many scientists, is that the mechanisms of correlated-electron SC in apparently different families are related¹⁻⁵. Among the many families of materials that have attracted attention in this context are organic charge-transfer solids (CTS), SC in which was found even before the copper oxides⁶. The proximity of SC to antiferromagnetism (AFM) in some, though not all (see below) CTS, have led to theories of SC in the CTS that are related to their counterparts in copper oxides⁷⁻¹⁵. Furthermore, the occurrence of SC in the CTS at fixed carrier density by application of pressure instead of doping has led to the belief that understanding CTS may be easier and a first step towards understanding correlated-electron SC itself. At the same time though, occurrence of SC at fixed carrier concentration demands that there is both broad and deep understanding of the role of this specific carrier concentration, and this issue has therefore been at the center of the discussions on organic SC, and is also the subject matter of the present work.

Two fundamentally different approaches to correlated-electron superconductivity in organic CTS exist in the literature. The first of these is specific to strongly dimerized quasi-two dimensional (quasi-2D) systems

such as κ -(BEDT-TTF)₂X (hereafter κ -(ET)₂X) and R[Pd(dmit)₂]₂ salts (here X and R are monovalent counteranion and countercation, respectively), in which pairs of cationic ET or anionic Pd(dmit)₂ molecules are strongly coupled as dimers, and the dimers form anisotropic triangular lattices (see Fig. 1)¹⁶. The charge on individual molecules is 0.5 and hence the dimer lattice has been considered as an *effective* $\frac{1}{2}$ -filled band with strong intradimer onsite Coulomb repulsion U_{eff} . Theoretical discussions are within the anisotropic triangular lattice Hubbard $U_{\text{eff}}-t-t'$ Hamiltonian, with hopping integrals t along \mathbf{x} and \mathbf{y} , and t' along the diagonal $\mathbf{y}-\mathbf{x}$ direction (see Fig. 1(b))^{7-10,13-15,17-22}. Metal-insulator transition occurs at a finite U_{eff}^c , with U_{eff}^c increasing with t' . For relatively small $|t'/t|$ the semiconducting state is AFM, while for moderate to large t' spin-liquid (SL) behavior is predicted. The theory gives satisfactory understanding of the magnetic behavior of CTS with small to moderate $|t'/t| < 1$, including AFM in κ -(ET)₂Cu[N(CN)₂]Cl (hereafter κ -Cl) with $|t'/t| \sim 0.44$ and apparent SL behavior in κ -(ET)₂Cu₂(CN)₃ (hereafter κ -CN) and β' -EtMe₃Sb[Pd(dmit)₂]₂ with $|t'/t| \sim 0.8 - 0.9$ ^{16,23}. Very recent experimental work²⁴ has concluded that the the simple SL picture as well as the $\frac{1}{2}$ -filled band Hubbard Hamiltonian are not appropriate for β' -EtMe₃Sb[Pd(dmit)₂]₂, a point to which we return later. Various mean field and dynamical mean field theory calculations find d -wave SC within the $\frac{1}{2}$ -filled $U_{\text{eff}}-t-t'$ model at intermediate $|t'/t|$, bounded by an antiferromagnetic semiconductor and a correlated metal in the phase diagram^{7-10,13-15,17-22}. Numerical investigations by us^{25,26} and others^{27,28} have, however, demonstrated

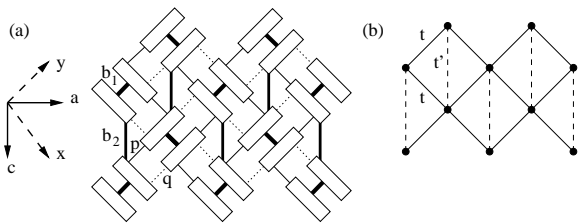


FIG. 1: (a) Lattice structure of the ET layer in κ -(ET) $_2$ X. The hopping integrals t_{b1} , t_{b2} , t_p , and t_q are indicated. (b) The effective $\frac{1}{2}$ -filled lattice: each dimer is now one lattice site. The effective hopping integrals $t = (|t_p| + |t_q|)/2$ and $t' = t_{b2}/2$.

that nonzero U_{eff} suppresses the long-range component of the superconducting pair-pair correlations, indicating absence of SC within the model. Additionally, the effective $\frac{1}{2}$ -filled band approach is inapplicable to CTS in which the organic monomer molecules are not coupled as dimers, and charge order (CO) and not AFM is proximate to SC^{29–33}.

An alternative theory^{5,34,35} ascribes each of the competing broken symmetries to the geometrically frustrated *monomer* lattice of organic molecules with carrier density $\rho = 0.5$ per molecule and bandfilling $\frac{1}{4}$. Although AFM and Mott insulating behavior are expected in the strongly dimerized and weakly frustrated $\rho = 0.5$ band, for stronger lattice frustration or weaker dimerization there is also a proximate static or dynamically fluctuating CO state, driven by quantum effects rather than classical electrostatics, that is a Wigner crystal of *spin-singlet pairs* (a paired electron crystal, hereafter PEC)^{36,37}. Uniquely to $\rho = 0.5$, it is possible to have a CO of spin-singlet pairs separated by pairs of vacant sites. Dipolar-spin coupling³⁸ and polar charge fluctuations³⁹ are related to dynamic CO fluctuations. Within the correlated $\frac{1}{4}$ -filled band theory, pressure-induced increased lattice frustration drives correlated motion of the spin-pairs into the “paired” vacant sites, giving a wavefunction that is still paired and constitutes the superconducting state^{5,34,35}. Our theory is at the interface of the resonating valence bond (RVB) theory⁴⁰ and the oldest version of the so-called bipolaron theory of superconductivity⁴¹. The spin-singlet bonds here arise from antiferromagnetic spin-coupling^{34,35}, as opposed to overly strong electron-phonon couplings, as assumed in the earlier literature⁴¹. We refer to this as the valence bond theory of SC, distinct from the RVB theory by its focus on $\rho = 0.5$.

The PEC concept is related to conjectures of “density wave of Cooper pairs” in the high T_c copper oxides^{42–48}, where the precise nature of the density wave is still being debated (see however, Reference 49). AFM is not the driver of SC within this second approach; SC in κ -(ET) $_2$ X is preceded by an “orbital reordering” that renders unequal charge densities on the monomers within a dimer unit, with mobile spin-singlet bonds forming between the charge-rich molecules of neighboring

dimers^{5,34,35,39}. Importantly, PEC formation is not limited to the dimerized κ -(ET) $_2$ X, and the CO phases adjacent to SC in undimerized α - β - and θ -(ET) $_2$ X are PECs⁵. This, in turn, indicates that the mechanism of SC in the dimerized and undimerized CTS is the same. Other calculations that have found SC within the $\frac{1}{4}$ -filled band Hubbard model using mean-field and random phase approximations^{39,50–52}, or variational Monte Carlo⁵³ are not filling-specific; a key aspect of our theory is that the PEC, and hence SC, are absent for bandfilling even modestly far from $\frac{1}{4}$.

In the present paper we discuss a new class of κ -CTS that are only now beginning to be investigated experimentally. These materials belong to the class $|t'/t| > 1$ and allow sharp comparisons between the two theoretical starting points described above, as we point out in the present work. We show that while within the effective $\frac{1}{2}$ -filled band theory neither the observed strange semiconductors nor superconductivity are expected, the ground state of the $\frac{1}{4}$ -filled Hubbard model is a strongly correlated metal that is susceptible to all the observed exotic transitions.

II. NEW QUASI-1D CTS AND THEORETICAL CHALLENGES

Until recently, SC in the κ -(ET) $_2$ X family was limited to materials which lie firmly in the $|t'/t| < 1$ region of the effective $\frac{1}{2}$ -filled Hubbard model. Discoveries of exotic behavior including SC in κ compounds with effective $|t'/t|$ significantly greater than 1 provide new testing grounds for the two classes of theories. The principal observations are given below.

(i) SL behavior has perhaps been seen in κ -(ET) $_2$ TaF $_6$ (hereafter κ -TaF $_6$)⁵⁴, with $|t'/t| > 1.5$. Absence of magnetic ordering has been demonstrated down to 1.6 K⁵⁴.

(ii) κ -(ET) $_2$ B(CN) $_4$ (hereafter κ -B(CN) $_4$) is an insulator at ambient pressure with effective $|t'/t| \sim 1.8$ ⁵⁵. It undergoes phase transition into a nonmagnetic state with spin-gap (SG)⁵⁵ at ~ 5 K. Raman measurements have failed to find CO so far, but the experiments were done only down to 10 K.

(iii) κ -(ET) $_2$ CF $_3$ SO $_3$ (hereafter κ -CF $_3$ SO $_3$) contains two inequivalent ET layers, labeled layers A and B, separated by the anion layer^{56,57}. Within the effective model $|t'/t| = 1.48$ (1.78) for layer A (B) at low temperatures⁵⁷. Following structural changes at 230 K and 190 K, AFM occurs at ambient pressure at a low Néel temperature T_N of 2.5 K⁵⁷. Transition to a metallic state and SC occurs under pressure ($T_{c,\text{max}} = 4.8$ K at 1.3 GPa)⁵⁷. $T_N < T_c$ (albeit pressure-induced) is unknown in any other correlated electron superconductor that has shown transition from AFM to SC.

The above observations defy explanations within the effective $\frac{1}{2}$ -filled band approach. First, even as magnetic measurements on κ -TaF $_6$ are awaited at lower temperatures (< 1.6 K), SL behavior is not expected within

the effective $\frac{1}{2}$ -filled band model for $|t'/t| \geq 1.5$. Theory limits the SL phase only to $|t'/t| \leq 1$ within the triangular lattice $\frac{1}{2}$ -filled Hubbard Hamiltonian^{58–60}. What is perhaps more relevant is that very recent experimental works^{24,61–63} have cast doubt on whether even κ -CN and EtMe₃Sb[Pd(dmit)₂]₂, which were thought to be prime candidates for SL in the parameter region $|t'/t| \leq 1$ until very recently¹⁶, should really be described as such. The original proponents of the SL picture for EtMe₃Sb[Pd(dmit)₂]₂, in particular, have found that the driver of the geometrical frustration here are hidden *charge and lattice fluctuations*, not expected within the simple $\frac{1}{2}$ -filled band Hubbard model²⁴.

Second, within the effective $\frac{1}{2}$ -filled band model, the SG transition observed in κ -B(CN)₄ can only be due to spin-Peierls transition, or due to a frustration-driven transition to a valence bond solid (VBS). The large ratio of inter-chain to intra-chain hopping, ~ 0.6 in κ -B(CN)₄, implies absence of 1D nesting necessary for the spin-Peierls transition characteristic of quasi-1D systems (note here that spin-density wave, and not the spin-Peierls state characterizes the spatial broken symmetry in (TMTSF)₂X where the same ratio at 0.2 is significantly smaller). It is also known from previous theoretical work that the Hubbard repulsion severely reduces bond dimerization in the 2D half-filled band even where nesting would have permitted this in the uncorrelated limit^{64,65}. The VBS is also precluded theoretically within the triangular lattice $\frac{1}{2}$ -filled band Hubbard model⁶⁶. We therefore conclude that the explanation of the SG transition in κ -B(CN)₄ requires going beyond the effective $\frac{1}{2}$ -filled band model.

Finally, the observed SC in κ -CF₃SO₃ also lies outside the domain of applicability of the effective $\frac{1}{2}$ -filled band theories. SC appears for significantly smaller $|t'/t| < 1$ within these theories^{7–10,13–15,17–22}. In the present paper we show from explicit numerical calculations based on the competing $\frac{1}{4}$ -filled band Hubbard model that the ground state of the latter is a strongly-correlated metal in which none of the above exotic phases are precluded, and hence any one of these can presumably dominate when small but nonzero interactions excluded in the purely electronic Hamiltonian are included. Superconducting correlations, in particular, are enhanced by the Hubbard U in the $\frac{1}{4}$ -filled band, relative to the noninteracting $U = 0$ limit, which is a necessary condition for correlated-electron SC.

III. THEORETICAL MODEL, PARAMETERS AND COMPUTATIONAL TECHNIQUES

We consider the Hubbard Hamiltonian for the κ lattice structure of Fig. 1(a),

$$H = \sum_{\langle ij \rangle, \sigma} t_{ij} (c_{i,\sigma}^\dagger c_{j,\sigma} + H.c.) + U \sum_i n_{i,\uparrow} n_{i,\downarrow}, \quad (1)$$

where $c_{i,\sigma}^\dagger$ ($c_{i,\sigma}$) creates (annihilates) an electron of spin σ on the highest molecular orbital of a *monomer* ET

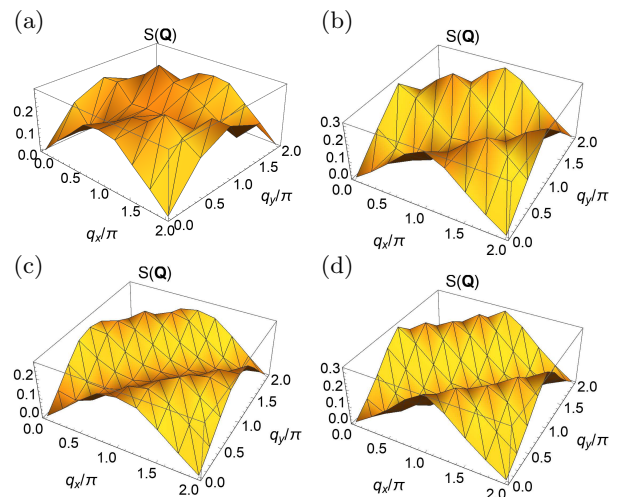


FIG. 2: (color online) Dimer spin structure factor $S(\mathbf{Q})$ for the κ -CF₃SO₃ lattice with $\rho = 1.5$ and $U=0.5$ eV. (a) 64 sites, layer A, (b) 64 sites, layer B, (c) 128 sites, layer A, and (d) 128 sites, layer B.

molecule i (hereafter “site”), and all other terms have their usual meanings. In our calculations for κ -CF₃SO₃ we take hopping integrals ($t_{b1}, t_{b2}, t_p, t_q; |t'/t|$) in eVs to be (0.234, 0.157, 0.029, -0.077; 1.48) and (0.248, 0.169, 0.048, -0.047; 1.78), for layers A and B, respectively⁵⁷. We report separate calculations for κ -B(CN)₄ with corresponding hopping parameters⁵⁵ (0.221, 0.117, 0.035, -0.029; 1.83). These parameters make κ -B(CN)₄ closer to 1D than κ -CF₃SO₃, as already noted above. These hopping integrals are for electrons and not holes; the corresponding carrier density is $\rho = 1.5$. Our zero temperature computational results are for finite periodic clusters with 32, 64, and 128 monomer sites⁶⁷ using the Path Integral Renormalization Group^{68,69} and Constrained Path Monte Carlo⁷⁰ methods⁶⁷. For both methods we fully incorporate lattice and spin-parity symmetries (see References 69 and 71), which significantly increases their accuracy. Our prior benchmark results of these methods are available in References 26, 34, and 35.

IV. COMPUTATIONAL RESULTS

A. Magnetic behavior

1. Weak AFM in κ -CF₃SO₃

The tendency to AFM is best discussed within the dimer representation³⁵. We define the total z -component of the spin on dimer i as

$$S_i^z = \frac{1}{2}(n_{i_1,\uparrow} + n_{i_2,\uparrow} - n_{i_1,\downarrow} - n_{i_2,\downarrow}). \quad (2)$$

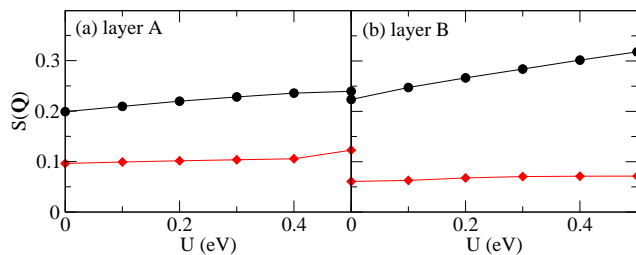


FIG. 3: (color online) $S(\mathbf{Q})$ versus U for a 128-site κ -CF₃SO₃ cluster. Circles and diamonds are for $\mathbf{Q}=(\pi,0)$ and (π,π) respectively.

In Eq. 2, i_1 and i_2 refer to the two different molecules within the dimer i and $n_{j,\sigma} = c_{j,\sigma}^\dagger c_{j,\sigma}$. We calculate the dimer spin structure factor,

$$S(\mathbf{Q}) = \frac{1}{N_d} \sum_{j,k} e^{i\mathbf{Q}\cdot(\mathbf{r}_j - \mathbf{r}_k)} \langle S_j^z S_k^z \rangle, \quad (3)$$

where N_d is the number of dimers and dimer position vectors \mathbf{r}_j are defined on a conventional square lattice, whose \mathbf{x} and \mathbf{y} axes are indicated in Fig. 1. Fig. 2 shows the \mathbf{Q} dependence at $\rho = 1.5$ of $S(\mathbf{Q})$ for 64 and 128 monomer lattice sites, separately for layers A and B in each case. The \mathbf{Q} dependence of $S(\mathbf{Q})$ here is similar to that of the $\frac{1}{2}$ -filled Hubbard model⁵⁹ with $|t'/t| > 1$. We find a line of maxima in $S(\mathbf{Q})$ perpendicular to the t' direction, with the dominant wavevector π along each chain. $S(\mathbf{Q})$ does not increase with system size, indicating the absence of long-range order. Fig. 3 shows that $S(\mathbf{Q})$ at $(\pi,0)$ is stronger than that at (π,π) in agreement with results for the $\frac{1}{2}$ -filled Hubbard model^{25,59,60}. $S(\pi,\pi)$ here is nearly half of that calculated by us previously for κ -Cl³⁵. The dominance of $S(\pi,0)$ over $S(\pi,\pi)$ is a consequence of quasi-1D character. Note however that in the 1D limit there is no long-range AFM. Additionally, the absence of true long range order in $S(\mathbf{Q})$ in our calculations indicates that κ -CF₃SO₃ is barely insulating and is close to a correlated metallic phase. The enhanced 1D character and the proximity to the metallic state, taken together, are the likely reasons for the small T_N in κ -CF₃SO₃.

2. Transition to the spin-gapped state in κ -B(CN)₄

As mentioned above, simple spin-Peierls transition or VBS formation, as have been suggested within the effective $\frac{1}{2}$ -filled model⁵⁵, cannot be the origin of the observed SG in κ -B(CN)₄⁶⁴⁻⁶⁶. The recent demonstration that the driving forces behind the apparent SL-like behavior in β' -EtMe₃Sb[Pd(dmit)₂]₂ are charge and lattice fluctuations²⁴, which are precluded in the $\frac{1}{2}$ -filled band but are *expected* within the $\frac{1}{4}$ -filled band characterization of the system⁵, gives a hint to the mechanism of the SG

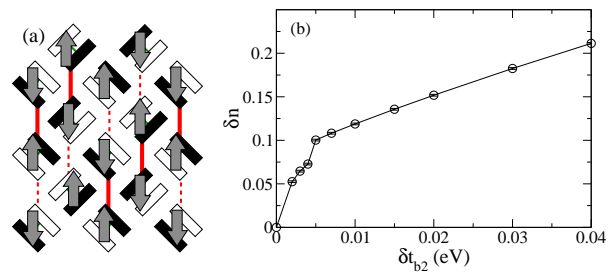


FIG. 4: (a) (color online) PEC accompanying bond alternation of t_{b2} bonds. Introducing the strong (solid red) and weak (dashed red) t_{b2} bonds leads to the indicated CO, where black and white boxes represent charge-rich and charge-poor ET molecules, respectively⁶⁷. Spins superimposed on the dimers represent the magnetic ordering in the $(\pi,0)$ antiferromagnetic phase. (b) 128 site CO order parameter, the difference in charge density between the charge-rich and the charge-poor molecules as a function of the difference in the t_{b2} hopping integrals. Calculations are for hopping parameters for κ -B(CN)₄ with $U=0.4$ eV.

in κ -B(CN)₄. Since similar intradimer charge inequalities can occur in all $\frac{1}{4}$ -filled band systems, we investigate the likelihood of PEC formation in the present case.

We have performed numerical calculations of charge densities in which the t_{b2} hopping integrals (see Fig. 1) alternate as $t_{b2}^0 \pm \delta t_{b2}$, as suggested in Reference 55. All other hopping parameters correspond to those for κ -B(CN)₄, given in Section III above. The PEC charge order pattern (Fig. 4(a)) appears *spontaneously* for nonzero δt_{b2} , as shown in Fig. 4(b), with CO $\dots 0110\dots$ along the bonds in the \mathbf{y} and \mathbf{x} -y directions, and $\dots 1010\dots$ along the bonds in the third direction \mathbf{x} (see Fig. 1(a) and Reference 67). Here ‘1’ and ‘0’ represent charge-rich and charge-poor molecules, respectively. Period doubling along both the crystal a and the c -axes are therefore expected at the SG transition, as opposed to only along t_{b2} ⁵⁵. Note that the pattern and phase of the CO is consistent with $(\pi,0)$ periodicity of the AFM, if we make the reasonable assumption of strong antiferromagnetic correlations between nearest neighbor charge-rich molecules.

Fig. 4(b) gives the calculated CO order parameter δn , the difference in the charge densities between the charge-rich and the charge-poor molecules. The kink at $\delta t_{b2} \sim 0.005$ eV is due to a level crossing; for $\delta t_{b2} > 0.005$ eV the difference in δn for 64 versus 128 sites is less than the size of the symbols in Fig. 4(b). We consider the range of δt_{b2} in Fig. 4(b) to be realistic⁵⁵, and while the calculated δn are small, they should be observable if experiments sensitive to the molecular charge are extended to $T < T_{SG}$. Even more importantly, we predict period doubling along *both* \mathbf{a} and \mathbf{c} -directions, consistent with PEC formation, that should also be experimentally verifiable.

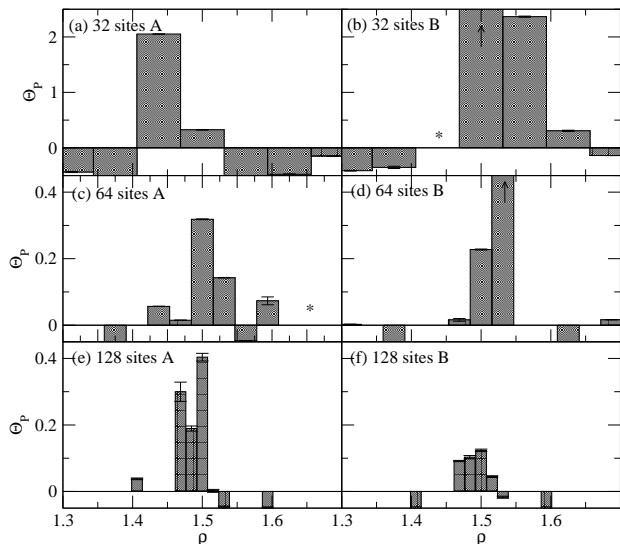


FIG. 5: The enhancement factor Θ_P for the long-range component of the pair-pair correlations with d_2 ($s + d_{x^2-y^2}$) symmetry, for hopping integrals corresponding to the κ -CF₃SO₃ lattice. $\Theta_P > 0$ implies pair-pair correlations enhanced over their $U = 0$ values. Pair-pair correlations are enhanced for a narrow region of carrier density $\rho = 1.5$ and are suppressed elsewhere (see text). Densities marked with * were removed due to finite-size effects⁶⁷. The computations for the 64- and 128-site clusters were done for density ranges narrower (1.3 - 1.7 and 1.4 - 1.6, respectively) than for the 32-site cluster based on previous work for $|t'/t| < 1$ that had shown peaking of Θ_P at $\rho = 1.5$.

B. Superconductivity: κ -CF₃SO₃ versus κ -B(CN)₄

1. Coulomb enhancement of superconducting correlations: κ -CF₃SO₃

We now probe the question of SC. As in previous work³⁵, calculations here are for variable carrier densities ρ , since the basic contention of our theory^{5,34,35} is that SC is specific to ρ exactly equal to or close to 1.5, and is absent in ρ even modestly far from 1.5. We calculate superconducting pair-pair correlations $P_{ij} = \langle \Delta_i^\dagger \Delta_j \rangle$, where Δ_i^\dagger creates a superposition of singlet pairs between monomer sites belonging to neighboring dimers. Such interdimer singlet pairs necessarily create unequal intradimer charge densities³⁵. Considering singlet pairs between monomer molecules on a central dimer and its six neighboring dimers, there occur four types of d -wave pairings (see Fig. 3 in Reference 35). The first of these pairing symmetries, d_1 , is similar to the usual $d_{x^2-y^2}$ symmetry and the second, d_2 , is a form of $s + d_{x^2-y^2}$ pairing also considered by other authors^{52,72,73}. For all three clusters we calculate the average long-range pair-pair correlations $\bar{P} = N_P^{-1} \sum_{|r_{ij}| > 2} P_{ij}$, where N_P is the number of terms in the sum with the restriction $r_{ij} > 2$ in units of dimer-dimer spacing³⁵. Since the minimal re-

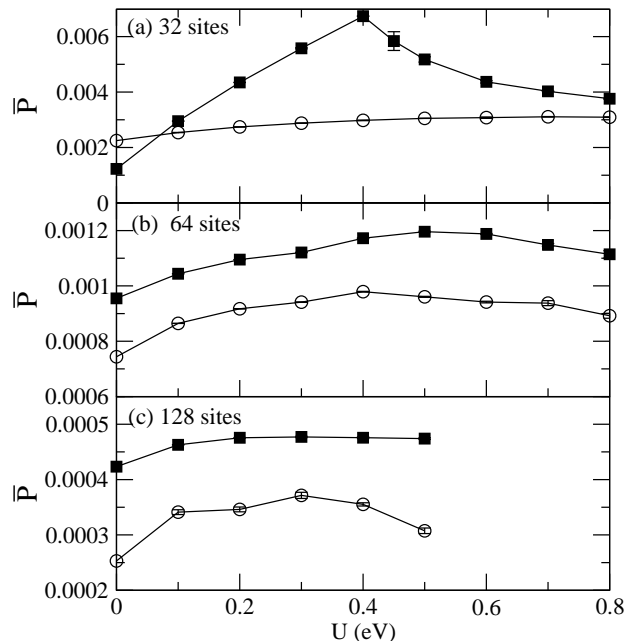


FIG. 6: Average long-range pair-pair correlation \bar{P} with d_2 ($s + d_{x^2-y^2}$) symmetry versus U for hopping parameters corresponding to κ -CF₃SO₃ at $\rho = 1.5$. Open (filled) symbols are for layer A (B).

quirement for interaction-driven SC is that nonzero Hubbard U enhances the pairing correlations, we calculate the enhancement factor $\Theta_P = [\bar{P}(U)/\bar{P}(U = 0)] - 1$. Then $\Theta_P > 0$ implies likelihood of pairing and $\Theta_P < 0$ indicates suppression of pairing by Hubbard U . Previous calculations³⁵ for effective $|t'/t| < 1$ found enhancement only for $\rho \sim 1.5$. A precise value for U for the actual materials is difficult to estimate. In the quasi-1D (TMTSF)₂X materials, $U \sim 1$ eV has been estimated for the extended Hubbard model⁷⁴. Based on the larger size of the ET molecule we expect a smaller U in the range 0.4 - 0.8 eV in κ -(ET)₂X compared to (TMTSF)₂X.

Our calculations find very strong enhancements of pair correlations with d_2 symmetry for $\rho \sim 1.5$ for both layers A and B of κ -CF₃SO₃, for all three cluster sizes (d_2 gave the most strongly enhanced pair correlations³⁵ also for κ -Cl and κ -CN). In Fig. 5 we show plots of $\Theta_P(d_2)$ versus ρ for all three cluster sizes, for $U = 0.4$ eV, separately for layers A and B in each case (see Supplementary Materials⁶⁷ for results on $\Theta_P(d_1)$). The calculated results are for a wide range of ρ in the 32 and 64-site clusters, spanning $\rho = 1.3 - 1.7$. A narrower density range 1.4 - 1.6 was considered for the 128-site cluster, based on the similar behavior of the three clusters. In spite of the quasi-1D character of the lattice, here we find nearly identical results as in the earlier work for the 2D lattice, where an even broader density range $\rho = 1.0 - 2.0$ was considered³⁵. In all cases we find that $\Theta_P(d_2) > 0$ occurs over a very narrow density range about 1.5. In Figs. 5(c) and (e) we see dips followed by rise in Θ_P for densities

close to but slightly away from density exactly 1.5. However, these dips and increases are tiny compared to the large peaks at density exactly at or very close to 1.5. The widths of the vertical shaded bars in Fig. 5 decrease with increasing lattice size, since between any two densities there are fewer total electron numbers in the smaller lattices. Importantly, (i) $\Theta_P(d_2) < 0$ outside of the density range 1.5 ± 0.1 in lattices larger than 32 sites, (ii) for all cases the largest enhancement in the pairing correlations is found either for ρ exactly equal to 1.5 or for an electron number immediately larger or smaller for a given lattice, and (iii) the range of densities over which pair correlations are enhanced by U decreases with increasing cluster size. Quantitatively speaking, the enhancements of the pair correlations for $\rho = 1.5$ here are either larger than (for 32 sites) or comparable to (for 64 sites)³⁵ those for effective $|t'/t| < 1$. Calculations for the very large 128-site clusters had not been performed before.

For the specific case of $\rho = 1.5$ we also performed calculations of the enhancement factor over a broad range of U for the 32- and 64-site clusters (see Fig. 6). For the 32 site layer B lattice a quantum phase transition occurs at $U \approx 0.4$ eV (see Fig. 6(a)). In this lattice at $U \approx 0.4$ eV a sharp increase in $S(\pi, \pi)$ coupled with a decrease in \bar{P} indicates a transition to an insulating antiferromagnetic state. This is a finite-size effect that is not present in larger lattices. On the other hand, this result does indicate that our strongly-correlated metal is close to an insulating phase, which would be likely a weak AFM, based on our calculations of the magnetic structure factor, see Section IV A.

2. Reduced tendency to superconductivity in κ -B(CN)₄

We have calculated U -dependent pair correlations also for the hopping parameters corresponding to κ -B(CN)₄, for clusters consisting of 32 monomer sites. We show these results in Figs. 7(a) and (b), where we have included the computational results for the 32-site κ -CF₃SO₃ lattice for comparison. The calculated pair-pair correlations are nearly identical for the two lattices for ρ far from 1.5 (Fig. 7(b)), where there is absence of enhancement, or even suppression of these correlations by the Hubbard U . The results for $\rho \sim 1.5$ (Fig. 7(a)) are noticeably different, however. On the one hand, the pair-pair correlations are enhanced by small Hubbard U for κ -B(CN)₄. On the other, the enhancement occurs over a significantly smaller range of U compared to that for κ -CF₃SO₃, with the peak in the enhancement occurring at very small ($\lesssim 0.2$ eV) U . For realistic molecular U (> 0.4 eV) the predicted tendency to SC in κ -B(CN)₄ is thus considerably smaller than in κ -CF₃SO₃.

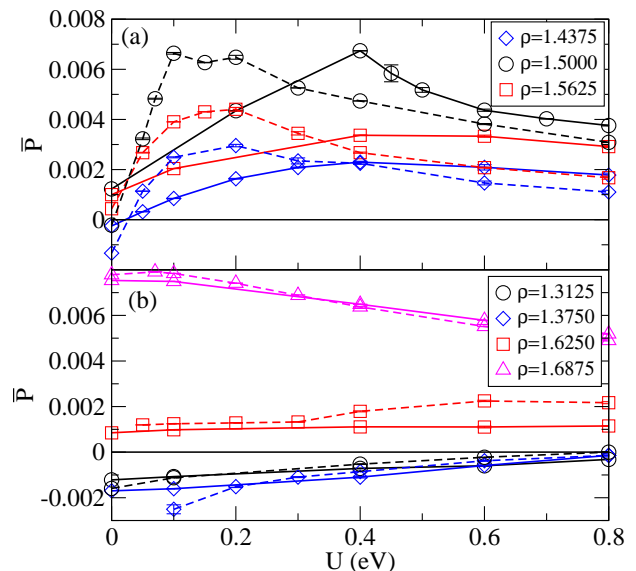


FIG. 7: (color online) Average long-range pair-pair correlation \bar{P} with d_2 ($s + d_{x^2-y^2}$) symmetry versus U for 32-site lattices. Solid (dashed) lines correspond to parameters for κ -CF₃SO₃ (κ -B(CN)₄). Panels (a) and (b) show densities near to and further from $\rho = 1.5$, respectively.

V. CONCLUSIONS

In summary, we have performed large scale accurate numerical calculations within the Hubbard Hamiltonian, for quasi-1D triangular lattice clusters of three different sizes, corresponding to the monomer κ -(ET)₂X lattice of Fig. 1(a), with realistic parameter values for κ -CF₃SO₃ and κ -B(CN)₄. Our results can be summarized as follows.

(i) For hopping parameters corresponding to both the inequivalent layers A and B of κ -CF₃SO₃, we find that $S(\mathbf{Q})$ peaks at $(\pi, 0)$ instead of (π, π) . This is in agreement with results obtained for the effective $\frac{1}{2}$ -filled band Hubbard model for $|t'/t| > 1$.

(ii) For hopping parameters corresponding to κ -B(CN)₄ we find the smallest alternation in t_{b2} , which has been suggested as the origin of the SG transition⁵⁵, is accompanied by CO as well as bond distortions in the two other directions, leading to period doublings. This is the classic signature of a tendency to unconditional transition to the PEC, noted previously for the effective $t' < t$ materials^{36,37}.

(iii) Returning to the hopping parameters corresponding to κ -CF₃SO₃, we find from electron density-dependent calculations on three different lattice sizes that superconducting pair-pair correlation functions of d_2 symmetry are enhanced by the Hubbard U only for density close to 1.5, precisely the carrier density in superconducting CTS. The superconducting symmetry is thus the same³⁵ as that for effective $|t'/t| < 1$. Also in agreement with previous calculations³⁵, for electron densities

even weakly away from 1.5 the Hubbard U suppresses pair correlations, indicating absence of SC here.

(iv) For hopping parameters corresponding to κ -B(CN)₄, similar electron density-dependent calculations for the 32-site cluster find enhancement of superconducting pair-pair correlation functions for $\rho = 1.5$, but only for U values smaller than the known Hubbard U for the ET molecule. This explains the absence of SC to date in this system, but also suggests that application of pressure, which would increase the bandwidth and decrease the effective $U/|t|$, can induce SC here. This predicted result is reminiscent of the experimental observation of high pressure-induced superconducting transition⁷⁵ from the spin-Peierls state in (TMTTF)₂PF₆, which is a PEC at the quasi-1D limit⁵.

The overall conclusion is that except for the weaker tendency to metal-insulator transition and AFM within the purely electronic Hamiltonian, which presumably is the reason behind the small T_N in κ -CF₃SO₃, all other behaviors at low temperatures are the same as what would be expected for the effective $|t'/t| < 1$. The fundamental reason for this is that the intradimer charge degrees of freedom become important at low temperatures in both κ -(ET)₂X and R[Pd(dmit)₂]₂. In recent years investigators have noted from different experimental studies on effective $|t'/t| < 1$ dimerized CTS that the lowest excitations in these involve intradimer charge fluctuations and the resultant lattice fluctuations^{61–63}. Here we note that the same is true for effective $|t'/t| > 1$. Should experiments at $T < 1.6$ K confirm the absence of magnetic long-range order in κ -TaF₆, this should be

ascribed also to intradimer charge fluctuations. The SG transition in κ -B(CN)₄ is likely due to PEC formation, as in the $|t'/t| < 1$ compound β -EtMe₃P[Pd(dmit)₂]₂^{5,24}. We suggest experiments sensitive to CO in κ -B(CN)₄.

Finally, the observation of SC in κ -CF₃SO₃ is a strong proof of the validity of our valence bond theory of SC. Elsewhere⁵ we have drawn attention to the very large number of disparate families of inorganic correlated-electron superconductors that share two features with CTS superconductors, viz., (a) $\frac{1}{4}$ -filling on frustrated lattices, and (b) SC proximate to unconventional charge-density waves. The very large number of such families suggests the universality of the proposed PEC-to-SC mechanism. Indeed, one of us has suggested the same mechanism of SC also for high T_c copper oxides, both hole and electron-doped, where an effective correlated $\frac{1}{4}$ -filled oxygen band is reached following a dopant-induced $\text{Cu}^{2+} \rightarrow \text{Cu}^{1+}$ valence transition⁴⁹.

VI. ACKNOWLEDGMENTS

S.M. acknowledges partial support from NSF-CHE-1764152. Some calculations in this work used the Extreme Science and Engineering Discovery Environment⁷⁶ (XSEDE), which is supported by National Science Foundation grant number ACI-1548562. Specifically, we used the Bridges system⁷⁷ which is supported by NSF award number ACI-1445606, at the Pittsburgh Supercomputing Center (PSC) under award TG-DMR190052.

* Electronic address: r.t.clay@msstate.edu

- ¹ R. H. McKenzie, *Science* **278**, 820 (1997).
- ² Y. Yanase, T. Jujo, T. Nomura, H. Ikeda, T. Hotta, and K. Yamada, *Phys. Rep.* **387**, 1 (2003).
- ³ E. Dagotto, *New J. Phys.* **7**, 67 (2005).
- ⁴ F. Steglich and S. Wirth, *Rep. Prog. Phys.* **79**, 084502 (2016).
- ⁵ R. T. Clay and S. Mazumdar, *Phys. Rep.* **788**, 1 (2019).
- ⁶ T. Ishiguro, K. Yamaji, and G. Saito, *Organic Superconductors* (Springer-Verlag, New York, 1998).
- ⁷ M. Vojta and E. Dagotto, *Phys. Rev. B* **59**, R713 (1999).
- ⁸ J. Schmalian, *Phys. Rev. Lett.* **81**, 4232 (1998).
- ⁹ H. Kino and H. Kontani, *J. Phys. Soc. Jpn.* **67**, 3691 (1998).
- ¹⁰ H. Kondo and T. Moriya, *J. Phys. Soc. Jpn.* **67**, 3695 (1998).
- ¹¹ B. J. Powell and R. H. McKenzie, *Phys. Rev. Lett.* **94**, 047004 (2005).
- ¹² J. Y. Gan, Y. Chen, Z. B. Su, and F. C. Zhang, *Phys. Rev. Lett.* **94**, 067005 (2005).
- ¹³ P. Sahebsara and D. S en echal, *Phys. Rev. Lett.* **97**, 257004 (2006).
- ¹⁴ T. Watanabe, H. Yokoyama, Y. Tanaka, and J. Inoue, *J. Phys. Soc. Jpn.* **75**, 074707 (2006).
- ¹⁵ C. D. Hebert, P. Semon, and A. M. S. Tremblay, *Phys. Rev. B* **92**, 195112 (2015).

- ¹⁶ K. Kanoda and R. Kato, *Annu. Rev. Condens. Matter Phys.* **2**, 167 (2011).
- ¹⁷ G. Baskaran, *Phys. Rev. Lett.* **90**, 197007 (2003).
- ¹⁸ J. Liu, J. Schmalian, and N. Trivedi, *Phys. Rev. Lett.* **94**, 127003 (2005).
- ¹⁹ B. Kyung and A. M. S. Tremblay, *Phys. Rev. Lett.* **97**, 046402 (2006).
- ²⁰ H. Yokoyama, M. Ogata, and Y. Tanaka, *J. Phys. Soc. Jpn.* **75**, 114706 (2006).
- ²¹ A. H. Nevidomskyy, C. Scheiber, D. S en echal, and A.-M. S. Tremblay, *Phys. Rev. B* **77**, 064427 (2008).
- ²² M. Sentef, P. Werner, E. Gull, and A. P. Kampf, *Phys. Rev. Lett.* **107**, 126401 (2011).
- ²³ H. C. Kandpal, I. Opahle, Y.-Z. Zhang, H. O. Jeschke, and R. Valent ı, *Phys. Rev. Lett.* **103**, 067004 (2009).
- ²⁴ T. Yamamoto, T. Fujimoto, T. Naito, Y. Nakazawa, M. Tamura, K. Yakushi, Y. Ikemoto, T. Moriwaki, and R. Kato, *Scientific Reports* **7**, 12930 (2017).
- ²⁵ R. T. Clay, H. Li, and S. Mazumdar, *Phys. Rev. Lett.* **101**, 166403 (2008).
- ²⁶ S. Dayal, R. T. Clay, and S. Mazumdar, *Phys. Rev. B* **85**, 165141 (2012).
- ²⁷ T. Watanabe, H. Yokoyama, Y. Tanaka, and J. Inoue, *Phys. Rev. B* **77**, 214505 (2008).
- ²⁸ T. Shirakawa, T. Tohyama, J. Kokalj, S. Sota, and S. Yunoki, *Phys. Rev. B* **96**, 205130 (2017).

- ²⁹ S. Kimura, H. Suzuki, T. Maejima, H. Mori, J. Yamaura, T. Kakiuchi, H. Sawa, and H. Moriyama, *J. Am. Chem. Soc.* **128**, 1456 (2006).
- ³⁰ H. Kobayashi, A. Kobayashi, and R. Kato, *Solid State Phys.* **21**, 826 (1986).
- ³¹ N. Tajima, A. Ebina-Tajima, M. Tamura, Y. Nishio, and K. Kajita, *J. Phys. Soc. Jpn.* **71**, 1832 (2002).
- ³² T. Yamamoto, Y. Nakazawa, M. Tamura, A. Nakao, Y. Ike-moto, T. Moriwaki, A. Fukaya, R. Kato, and K. Yakushi, *J. Phys. Soc. Jpn.* **80**, 123709 (2011).
- ³³ T. Shikama, T. Shimokawa, S. Lee, T. Isono, A. Ueda, K. Takahashi, A. Nakao, R. Kumai, H. Nakao, K. Kobayashi, et al., *Crystals* **2**, 1502 (2012).
- ³⁴ N. Gomes, W. W. De Silva, T. Dutta, R. T. Clay, and S. Mazumdar, *Phys. Rev. B* **93**, 165110 (2016).
- ³⁵ W. W. De Silva, N. Gomes, S. Mazumdar, and R. T. Clay, *Phys. Rev. B* **93**, 205111 (2016).
- ³⁶ H. Li, R. T. Clay, and S. Mazumdar, *J. Phys.: Condens. Matter* **22**, 272201 (2010).
- ³⁷ S. Dayal, R. T. Clay, H. Li, and S. Mazumdar, *Phys. Rev. B* **83**, 245106 (2011).
- ³⁸ C. Hotta, *Phys. Rev. B* **82**, 241104(R) (2010).
- ³⁹ A. Sekine, J. Nasu, and S. Ishihara, *Phys. Rev. B* **87**, 085133 (2013).
- ⁴⁰ P. W. Anderson, *Science* **235**, 1196 (1987).
- ⁴¹ B. K. Chakraverty and J. Ranninger, *Phil. Mag. B* **52**, 669 (1985).
- ⁴² M. Franz, *Science* **305**, 1410 (2004).
- ⁴³ Z. Tesanovic, *Phys. Rev. Lett.* **93**, 217004 (2004).
- ⁴⁴ H.-D. Chen, O. Vafek, A. Yazdani, and S.-C. Zhang, *Phys. Rev. Lett.* **93**, 187002 (2004).
- ⁴⁵ M. Vojta and O. Rösch, *Phys. Rev. B* **77**, 094504 (2008).
- ⁴⁶ M. H. Hamidian, S. D. Edkins, S. H. Joo, A. Kostin, H. Eisaki, S. Uchida, M. J. Lawler, E.-A. Kim, A. P. Mackenzie, K. Fujita, et al., *Nature* **532**, 343 (2016).
- ⁴⁷ P. Cai, W. Ruan, Y. Peng, C. Ye, X. Li, Z. Hao, X. Zhou, D.-H. Lee, and Y. Wang, *Proc. Natl. Acad. Sci.* **12**, 1047 (2016).
- ⁴⁸ A. Mesaros, K. Fujita, S. D. Edkins, M. H. Hamidian, H. Eisaki, S. Uchida, J. C. S. Davis, M. J. Lawler, and E.-A. Kim, *Proc. Natl. Acad. Sci.* **113**, 1266112666 (2016).
- ⁴⁹ S. Mazumdar, *Phys. Rev. B* **98**, 205153 (2018).
- ⁵⁰ H. Kondo and T. Moriya, *J. Phys. Soc. Jpn.* **70**, 2800 (2001).
- ⁵¹ K. Kuroki, *J. Phys. Soc. Jpn.* **75**, 051013 (2006).
- ⁵² D. Guterding, M. Altmeyer, H. O. Jeschke, and R. Valentí, *Phys. Rev. B* **94**, 024515 (2016).
- ⁵³ H. Watanabe, H. Seo, and S. Yunoki, *Nature Comm.* **10**, 3167 (2019).
- ⁵⁴ T. Kawamoto, K. Kurata, and T. Mori, *J. Phys. Soc. Jpn.* **87**, 083703 (2018).
- ⁵⁵ Y. Yoshida, H. Ito, M. Maesato, Y. Shimizu, H. Hayama, T. Hiramatsu, Y. Nakamura, H. Kishida, T. Koretsune, C. Hotta, et al., *Nat. Phys.* **11**, 679 (2015).
- ⁵⁶ M. Fettouhi, L. Ouahab, C. Gomez-Garcia, L. Ducasse, and P. Delhaes, *Synth. Metals* **70**, 1131 (1995).
- ⁵⁷ H. Ito, T. Asai, Y. Shimizu, H. Hayama, Y. Yoshida, and G. Saito, *Phys. Rev. B* **94**, 020503(R) (2016).
- ⁵⁸ T. Yoshioka, A. Koga, and N. Kawakami, *Phys. Rev. Lett.* **103**, 036401 (2009).
- ⁵⁹ L. F. Tocchio, C. Gros, R. Valentí, and F. Becca, *Phys. Rev. B* **89**, 235107 (2014).
- ⁶⁰ S. Acheche, A. Reymbaut, M. Charlebois, D. Sénéchal, and A.-M. S. Tremblay, *Phys. Rev. B* **94**, 245133 (2016).
- ⁶¹ K. Itoh, H. Itoh, M. Naka, S. Saito, I. Hosako, N. Yoneyama, S. Ishihara, T. Sasaki, and S. Iwai, *Phys. Rev. Lett.* **110**, 106401 (2013).
- ⁶² K. Yakushi, K. Yamamoto, T. Yamamoto, Y. Saito, and A. Kawamoto, *J. Phys. Soc. Jpn.* **84**, 084711 (2015).
- ⁶³ S. Fujiyama and R. Kato, *Phys. Rev. B* **97**, 035131 (2018).
- ⁶⁴ S. Mazumdar, *Phys. Rev. B* **36**, 7190 (1987).
- ⁶⁵ J. C. Pillay, K. Wierschem, and P. Sengupta, *Phys. Rev. B* **88**, 054416 (2013).
- ⁶⁶ N. Gomes, R. T. Clay, and S. Mazumdar, *J. Phys. Condens. Matter* **25**, 385603 (2013).
- ⁶⁷ See Supplemental Material at <http://link.aps.org/supplemental/xx.xxxx> for further details of calculations.
- ⁶⁸ T. Kashima and M. Imada, *J. Phys. Soc. Jpn.* **70**, 2287 (2001).
- ⁶⁹ T. Mizusaki and M. Imada, *Phys. Rev. B* **69**, 125110 (2004).
- ⁷⁰ S. Zhang, J. Carlson, and J. E. Gubernatis, *Phys. Rev. B* **55**, 7464 (1997).
- ⁷¹ H. Shi, C. A. Jimenez-Hoyos, R. Rodriguez-Guzman, G. E. Scuseria, and S. Zhang, *Phys. Rev. B* **89**, 125129 (2014).
- ⁷² D. Guterding, S. Diehl, M. Altmeyer, T. Methfessel, U. Tutsch, H. Schubert, M. Lang, J. Müller, M. Huth, H. O. Jeschke, et al., *Phys. Rev. Lett.* **116**, 237001 (2016).
- ⁷³ H. Watanabe, H. Seo, and S. Yunoki, *J. Phys. Soc. Jpn.* **86**, 033703 (2017).
- ⁷⁴ F. Mila, *Phys. Rev. B* **52**, 4788 (1995).
- ⁷⁵ T. Adachi, E. Ojima, K. Kato, H. Kobayashi, T. Miyazaki, M. Tokumoto, and A. Kobayashi, *J. Am. Chem. Soc.* **122**, 3238 (2000).
- ⁷⁶ J. Towns, T. Cockerill, M. Dahan, I. Foster, K. Gauthier, A. Grimshaw, V. Hazlewood, S. Lathrop, D. Lifka, G. D. Peterson, et al., *Computing in Science & Engineering* **16**, 62 (2014).
- ⁷⁷ N. A. Nystrom, M. J. Levine, R. Z. Roskies, and J. R. Scott, in *Proceedings of the 2015 XSEDE Conference: Scientific Advancements Enabled by Enhanced Cyberinfrastructure* (ACM, New York, NY, USA, 2015), XSEDE '15, pp. 30:1–30:8, ISBN 978-1-4503-3720-5.